STEERING COLUMN TILT LEVER - P/M MATERIAL DEVELOPMENT

W. Brian James*, Vernon C. Pottert, and Thomas F. Murphy *

Hoeganaes Corporation
Riverton NJ

The Presmet Corporation
Worcester MA

Paper presented at the 1990 SAE International Congress and Exposition, Coho Hall, Detroit, MI, February 27,1990. SAE Technical Paper 900381.

ABSTRACT

Automotive steering columns use a variety of levers to lock the flit mechanism in position. A new P/M material has been developed to withstand the impact and hardness performance requirements of this application. The new material is currently subjected to a brief surface carburizing and tempering treatment to impart wear resistance. The P/M part only requires honing of the pivot hole to meet the specified tolerance.

Long term plans are to achieve the desired performance requirements using a modified version of the new P/M material, with a higher graphite addition, which can be used after tempering the" as-sintered" product.

The Charpy impact properties of three P/M materials, each based on a partially alloyed powder (Distaloy 4800A) but with different percentages of added graphite, have been tested for a variety of processing conditions. Neutral hardening, carburizing, and sinter-hardening treatments have been compared. The influence of tempering temperature and the incorporation of a cryogenic treatment in the process cycle have been reviewed. Quantitative metallography has been used to compare the pore size, pore shape, and percentage of microstructural constituents present in the different P/M materials. The measured impact properties are discussed in relation to these factors.

INTRODUCTION

Three powder metallurgy parts are used in the steering column illustrated in Figure 1. Two are flit levers that permit adjustment of the column into one of five possible positions while the third part is a column lock lever. The tilt levers need to have adequate tensile strength and a surface hardness that will resist brinelling and wear of the grooved profile area. In addition, the pans should have a tough core because they are subjected to impact loading during adjustment of the steering column.

The tilt levers are illustrated in greater detail in Figure 2. Their shape complexity is such that they would be expensive to machine. However, they are well suited to production as powder metallurgy parts.

Powder metallurgy processing permits the microstructure of the pan to be tailored to the demands of the application. The microstructural constituents have a significant

effect on the mechanical properties of the material. In order to optimize the performance, the correct balance must be achieved between the microstructure of the inner and interparticle regions (1,2).

High temperature sintering of 8 - 10% nickel steel has been used to produce the tilt levers. However, because the specified tolerances could not be held following high temperature sintering, these sinter-hardened parts required honing of the pivot hole and grinding of the grooves to achieve the desired parallelism.

A new material and P/M process route that has been develop, for making the tilt levels is described in this paper. The new material is given a brief surface carburizing treatment to impart wear resistance.

Parts made by the new process route only require honing of the pivot hole to meet the specified tolerance.

Attempts are currently underway to develop material, and process routes that will eliminate the need to surface carburize the tilt levers. The preliminary results of this program are also presented.

EXPERIMENTAL PROCEDURE

Materials

A partially alloyed powder, Distaloy 4800A, was used as the base for the premixes. An additional two- percent of elemental nickel powder (Inco 123) was admixed with the Distaloy base. Three premixes were prepared and each contained 0.75 % Acrawax for lubrication. The mixes contained different amounts of graphite (0.3,0.6 and 0.8 %) as summarized in Table 1.
The three mixes were used to produce four groups of samples A, B, C, and D. Groups A and B contained the same amount of graphite (0.3%) and were both quench-hardened in oil. The samples in group B were given a brief surface carburizing treatment whereas those in group A were given a neutral hardening cycle in which the carbon potential of the furnace atmosphere was similar to the carbon content of the parts. The parts in-groups C and D were produced from the mixes with higher graphite additions (0.6 and 0.8% respectively). These parts were not quench-hardened but were used" as-sintered "in what we have termed the" sinter-hardened "condition.

Compaction and Sintering

Rectangular unnotched Charpy impact bars (10 mm x 10 mm cross-section) were compacted to a density
of 6.9 g/cm^3. The bars were pre-sintering at 816 °C (1500 °F) and repressed to a density of 7.3 g/cm^3. The bars were sintered in a production furnace at 1127. °C (2060 °F) in a nitrogen / hydrogen atmosphere (10 % hydrogen) to which methane was added to achieve the desired carbon potential. The belt speed was two minutes / foot which equates to approximately 15 minutes at temperature.

The bars produced from the premix with 0.3 % graphite were divided into two groups

for subsequent heat treatment:

- Group A was given a neutral hardening cycle which consisted of austenitizing at 816 °C (1500°F) for 30 minutes in an endothermic atmosphere with a carbon potential of 0.45 % followed by oil quenching.

- Group B was hardened by austenitizing at 816 °C (1500 °F) for 15 minutes in an endothermic atmosphere with a carbon potential of 0.8 % followed by oil quenching. This treatment gave the bars a case with about 0.8% carbon.

The bars produced from the premixes with 0.6 and 0.8 % graphite, groups C and D respectively, were not subjected to an austenitizing and quenching treatment. These bars were tested in the "sinter-hardened" condition.

The groups of bars were further subdivided prior to tempering at 177,232, or 316 °C (350,450, or 600 °F). Selected subgroups were given a second temper or subjected to a cryogenic treatment prior to a second temper.

The tempering cycles were for one hour at the designated temperature and cryogenic treatment was at 840(2 (- 120 OF) for 3 hours.

The various processing treatments are summarized in Table 2 along with a description of the thermal treatment of the samples from groups A, B, C, and D.

Impact Testing.

Room temperature impact testing of the unnotched Charpy bars was carried out according to the procedure described in ASTM E 23. Five bars were tested from each material and processing condition. Rockwell superficial hardness was determined for the various samples according to the procedure described in ASTM E 18.

Metallographic Examination

Sample cross-sections were cut from the impact test specimens and prepared for metallographic examination. All Metallographic preparation was done on a Struers Abrapoi automated grinder/polisher. Automated polishing is essential to provide the high quality scratch-free and stain-flee surface required for quantitative metallography.

Pore size and shape measurements were carried out using a Leitz TAS-Plus automated image analyzer. Pores were sized according to their area using size intervals ranging from 0-100 gm^2 to 2400-2500 gm^2. (A circular pore with a diameter of 50 μm will have an area of 1963 μm^2. To have an area of 100 μm^2 a circular pore would have a diameter of approximately 11 μm). Pore shape was assessed using the parameter $4\pi A/P^2$, where A is the area and P the perimeter. For a perfectly circular pore $4\pi A/P^2 = 1$. Irregularly shaped pores will have values of less than 1 for this parameter.

A 10 x 10 field meander was used to samplel00 fields representing a total area of 4.7 nun^2. In order to ensure that only whole pores were used in the analysis,

measurements were made on detected pores in an area at the upper left corner of the screen (the guard frame) representing approximately one third of the measuring frame. Pores touching the outside edges of the guard or measuring frame were removed from the analysis. Those touching the inside edges of the guard flame were reconstructed and included in the assessment. This procedure prevents the analysis being biased towards the smaller pores, which would have occurred had only pores touching the outside edges been removed. For pore shape assessment, pores smaller than 4μm in length (maximum Feret's diameter) were eliminated from the analysis. This was done by skeletonization and end point removal and not by erosion which could segment the pores or size them according to their minimum dimension.

The samples were then etched with a combination of 2 % nickel / 4 % picral prior to carrying out a quantitative estimate of their microstructural constituents. For the quenched and tempered samples this was relatively straightforward. However before this could be done for the sinter-hardened samples, a decision had to be made concerning which microstructural features should be included in the analysis. This decision was aided by the use of semi-quantitative X-ray analysis on a scanning electron microscope. Energy dispersive analysis was used to compare the relative concentrations of nickel, copper, and molybdenum in selected microstructural features; pearlite, the ferrite rim surrounding many pearlite colonies, and the non-etching nickel rich areas in the interparticle regions. The pearlitic areas were relatively free of nickel and molybdenum and contained less than 1% copper. The ferrite rim around many pearlite colonies contained about 1% copper, and 1 - 4 % nickel. The non-etching nickel rich areas in the interparticle regions were found to contain 5 - 40 % nickel, 1 - 3 % copper, and 0.5 - 2 % molybdenum. The nickel concentration in these regions was also estimated using wavelength spectroscopy on a SEM. A spot analysis was carried out at 25 kV and a magnification of 3000 X. 'Ibis showed the nickel concentration to vary from less than 0.5 % in the pearlite to just over 1% in the ferrite rim and from 10 - 20 % in the non-etching nickel rich areas.

It was therefore decided to assess the percentages of the following microstructural constituents:

- pearlite
- ferrite
- nickel rich ferrite (containing divorced carbides)
- bahrite
- nickel rich non-etching regions
- martensite (dark etching - found in quench-hardened samples)
- dark etching martensitc plus retained austenite
- light etching martensite plus retained austenite
- porosity

These features are illustrated in Figures 3 - 7. The light etching martensite in the sinter-hardened samples contains a higher nickel concentration than the dark etching martensite. Vickers microhardness measurements were also made within such features in selected samples and the results are shown alongside Figures 3 - 7.

A quantitative point count estimate of the percentage of the microstructural

constituents present in selected samples was carried out using a 20 point grid (with a point spacing of 20 mm) at a magnification of 750 diameters. Twenty random fields were examined per sample and the average results reported.

RESULTS

Impact test results are summarized in Table 3 and hardness data in Table 4. The results of pore size and pore shape analysis are presented in Figure 8 and the estimates of the percentages of different microstructural constituents present in the various samples are summarized in Table 5.

DISCUSSION

Partially Alloyed Powder

The mechanical properties of P/M materials are directly related to their microstructure and the porosity (amount, size, distribution, and morphology) they contain. Alloying additions are made to develop specific material performance characteristics. However, the manner in which the alloys are constituted has a significant effect on the porosity and the microstructure of the final product (1,3}.

Partially alloyed or diffusion bonded powders sold under the name Distaloy® have been used for quite some time for the production of high strength sintered components. The production of these powders involves the heat treatment of a mixture of iron powder and alloying elements in a reducing atmosphere. During this treatment, the alloying elements partially diffuse into the iron powder and a metallurgical bond is achieved.

There are a number of advantages associated with this approach to alloying. Because the alloying elements are only partially alloyed, the high compressibility of the base iron is maintained and the green strength is increased. Fine powders of the alloying elements can be added to the iron powder with reduced risk of segregation and dusting during transport and handling of the powder mix. Segregation may lead to compositional variations within parts and from part to part, which may contribute to variation in dimensional change during sintering. Dusting leads to loss of alloying additions with a resultant reduction in petrol, since and .may also contribute to variation in dimensional change during sintering. Reduced segregation and dusting makes it easier for the parts producer to consistently meet close dimensional tolerance requirements.

Diffusion bonding the fine particle size alloying elements to the base iron reduces their tendency to forth lumps or agglomerates during subsequent mixing with graphite and lubricant. The alloying additives will thus be more evenly distributed on a macroscopic scale. The microstructure of materials produced from partially alloyed powders will, however, be heterogeneous as illustrated in Figures 3 - 7, and they will not exhibit uniform hardness unless they are sintered at very high temperatures for long limes.

It is the dimensional stability of the Distaloy base powder that is critical to the present application. Distaloy materials also have good impact performance. Advantage is taken of the heterogeneous microstructure resulting from the partially alloyed base and

additional nickel is admixed to increase the toughness of the interparticle regions.

Microstructure

It has been shown that the impact performance of P/M materials is directly related to density (4). In the present study, the density has been fixed and the influence of microstructure has been assessed. The compaction and sintering sequence was similar for all four groups of samples and there were no significant differences observed in pore size or pore shape between the samples (Figure 8).

The primary difference between the groups was that groups A and B were quench-hardened whereas groups C and D were sinter-hardened. This resulted in some major microstructural differences. The quenched and tempered samples (A and B) contained 50 - 60 % martensite, about 10 % bainite, and 20 - 25 % non-etching nickel rich areas. The sinter-hardened samples contained about 25 - 30 % pearlite, 20 - 25 % nickel rich ferrite and ferrite, 20 - 25 % non-etching nickel rich areas, plus 15 - 25 % martensite (dark and light etching). The higher carbon content samples contained a slightly higher percentage of pearlite and proportionally less ferrite.

Impact and Hardness

The specification requires the parts to have impact absorption energy of 27.2 J (20-ft. lb.) and a surface hardness of 68 HR15N. It can be seen from Tables 3 and 4 that, while the sinter-hardened samples have better impact properties than the quench hardened samples, they are marginal with respect to hardness.

Groups A and B are comparable in performance. The hardness and impact values for group B are slightly higher because of their slightly bigger carbon content - a result of the short surface carburizing treatment applied to give wear resistance. Tempering improves the impact performance compared with that of the as quenched samples. However, there appears to be no benefit of tempering above 232 °C (450 °F) as the impact energy and hardness both decrease at a tempering temperature of 316 °C (600 °F) - Figures 9 and 10. It is interesting to note that the best impact performance in-group A and B was obtained from the as sintered samples. These samples were however below the specified hardness.

Double tempering does not appear to provide sufficient benefit to make it an attractive processing option. Cryogenic treatment does not improve impact performance either although it does increase hardness -Figures 11 and 12. The martensite regions of the quench-hardened samples contain a significant amount of retained austenite and double tempering, with or without cryogenic treatment, will convert some of the retained austenite to tempered martensite.

The Effect of Microstructure on Impact and Hardness Values

The samples from groups C and D have noticeably better impact properties than those from groups A and B. Their impact performance is, in most cases, more than double the specified minimum of 27.2 $. However, the parts are marginal with respect to the hardness specification of 68 HR15N. While these sinter-hardened samples contain a

similar amount of the non-etching nickel rich areas they do not contain the same percentage of martensite - Figures 13 andl4. In place of the martensite are regions of pearlite and nickel rich ferrite, which, although they do not impart the same hardness as the martensite, are somewhat tougher. In view of the reduced amount of martensite and retained anstenite ha these samples double tempering, with or without cryogenic treatment would be expected to have little effect on performance. Cryogenic treatment does however increase part hardness; particularly ha the samples from group D - Figure 12. Tempering at 232-°C (450^{0}F) appears to be best with respect to impact performance and hardness.

Sinter-hardened Samples: The Effect of Extended Sintering Time

While the sinter-hardened samples have good impact properties they are marginal with respect to meeting the specified hardness requirement. It was thought that increased diffusion of the alloying elements might improve the hardness. Samples from the C and D groups that had been sintered using a belt speed of two minutes / foot (equivalent to about 15 minutes at temperature) were sintered for a second time but at a belt speed of four minutes / foot. These samples were therefore given about 45 minutes at the sintering temperature. The test bars were tempered at 177-°C (350-°F) prior to impact testing. Impact values of 58.5 J (43-ft. lb.) and 55.8 J (41-ft. lb.) were measured for the 0.6 and 0.8 % graphite samples respectively. The corresponding hardness results of 70 and 73.5 HR15N were above the specification minimum of 68 HR15N.

Quantitative microscopy showed that the increased sintering time resulted ha a greater percentage of martensite in these sinter-hardened samples - Figure 16. The martensite formation was a consequence of increased diffusion of the alloying elements. The percentage of non-etching nickel rich regions decreased and the locally enhanced hardenability led to the formation of martensite rather than pearlite and nickel rich lexrite. The extended sintering time increased the roundness of the pores compared with those ha the original samples examined - Figure 17. The pore size was not particularly affected - Figure 18. The increased pore roundness may improve the fatigue performance of the material but does not appear to have much effect on impact absorption energy (1).

The impact and hardness required in steering column tilt levers can be achieved by quench-hardening and tempering a material based on Distaloy 4800A to which 2% nickel and 0.3% graphite have been added. There is little or no benefit to be gained from a double tempering treatment, with or without cryogenic treatment. Sinter-hardened materials resulted ha better impact performance but were marginal with respect to hardness. Extended sintering trials with sinter-hardened materials were, however, promising.

Steering column tilt levers are currently made by double pressing a partially alloyed (Distaloy) based material to a density of 7.3 g/cm^3 to produce parts with impact and hardness values ha excess of the specified minimum (27.2 J and 68 HR15N respectively). The parts are given a brief carburizing treatment and tempered at 232°C (450°F) to provide a wear resistant surface. This cost-effective approach to making these parts eliminates the need to machine the selector grooves and the only

machining required is honing of the pivot hole.

The powder mix used to make the tilt levers is prepared using the AncorBond® process, a patented premixing method for reducing dusting and segregation (5). This results in even greater part to part consistency and although a premium grade, high performance powder base and premixing method are used, the overall process is a more cost effective way to make these parts than high temperature sintering an 8 – 10 % nickel steel.

Work in progress indicates that it is possible to increase the impact performance of the tilt levers by sinter hardening rather than quench hardening the parts. Additional experiments are required to optimize the time at sintering temperature and the cooling rate from sintering temperature for this alternative process route.

ACKNOWLEDGEMENTS

The authors would like to thank G. J. Golin of the Hoeganaes Corporation for carrying out the quantitative estimate of the microstructural constituents in selected samples.

1. W. B. James," Fatigue Properties of Ferrous P/M Materials ", presented at P/M Seminar, São Paulo, Brazil, October 1989.

2. T. Saito and M. Obayashi," High Strength Sintered Steel Without Heat Treatment ", Modem Developments in Powder Metallurgy, Vol. 21,1988, p. 197, published by MPIF, Princeton NJ.

3. W. B. James," Alloying Methods for High Performance, Ferrous Powder Metallurgy Parts ", presented at P/M Seminar, São Paulo, Brazil, October, 1989.

4. R. C. O'Brien," Impact and Fatigue Characterization of Selected Ferrous P/M Materials ", Progress in Powder Metallurgy, Vol. 43,1987, p. 749, published by MPIF, Princeton NJ.

5. F. J. Semel, "Properties of Parts Made from an AncorBond® Processed Carbon-Nickel-Steel Powder Mix (FN-0208) ", Advances in Powder Metallurgy, Volume 1, 1989, p 9, published by MPIF, Princeton NJ.

	GROUP A	GROUP B	GROUP C	GROUP D
NICKEL	2.0	2.0	2.0	2.0
GRAPHITE	0.3	0.3	0.6	0.8
ACRAWAX	0.75	0.75	0.75	0.75
DISTALOY 4800A	balance	balance	balance	balance

	NICKEL	MOLYBDENUM	COPPER	IRON
DISTALOY 4800A (typical chemistry)	4.0	0.5	1.5	balance

TABLE 1 : Chemistry of the materials used to prepare the samples

SAMPLE TREATMENT	GROUP A	GROUP B	GROUP C	GROUP D
AS SINTERED	AS	BS	CS	DS
QUENCHED	AH	BH	X	X
QUENCH & TEMPER 177 °C	AH3	BH3	CS3	DS3
QUENCH & TEMPER 232 °C	AH4	BH4	CS4	DS4
QUENCH & TEMPER 316 °C	AH6	BH6	CS6	DS6
QUENCH & TEMPER 177 °C/177 °C	AH3-3	BH3-3	CS3-3	DS3-3
QUENCH & TEMPER 177 °C/232 °C	AH3-4	BH3-4	CS3-4	DS3-4
QUENCH & TEMPER 177 °C/316 °C	AH3-6	BH3-6	CS3-6	DS3-6
QUENCH & TEMPER 232 °C/177 °C	AH4-3	BH4-3	CS4-3	DS4-3
QUENCH & TEMPER 232 °C/232 °C	AH4-4	BH4-4	CS4-4	DS4-4
QUENCH & TEMPER 232 °C/316 °C	AH4-6	BH4-6	CS4-6	DS4-6
QUENCH & TEMPER 177 °C/FREEZE/TEMPER 177 °C	AH3-F-3	BH3-F-3	CS3-F-3	DS3-F-3
QUENCH & TEMPER 177 °C/FREEZE/TEMPER 232 °C	AH3-F-4	BH3-F-4	CS3-F-4	DS3-F-4
QUENCH & TEMPER 177 °C/FREEZE/TEMPER 316 °C	AH3-F-6	BH3-F-6	CS3-F-6	DS3-F-6
QUENCH & TEMPER 232 °C/FREEZE/TEMPER 177 °C	AH4-F-3	BH4-F-3	CS4-F-3	DS4-F-3
QUENCH & TEMPER 232 °C/FREEZE/TEMPER 232 °C	AH4-F-4	BH4-F-4	CS4-F-4	DS4-F-4
QUENCH & TEMPER 232 °C/FREEZE/TEMPER 316 °C	AH4-F-6	BH4-F-6	CS4-F-6	DS4-F-6

TABLE 2 : Sample identification and summary of processing conditions .

SAMPLE	GROUP A	GROUP B	GROUP C	GROUP D
S	65.6	65.6	69.8	69.4
H	80.8	81.3	X	X
3	79.0	77.6	67.8	68.5
4	77.8	76.9	67.4	67.6
6	73.3	73.4	66.1	67.2

SAMPLE	PEARLITE	FERRITE	NICKEL RICH FERRITE	BAINITE	NICKEL RICH NON ETCHING	MARTENSITE	DARK ETCHING MARTENSITE	LIGHT ETCHING MARTENSITE	POROSITY
A S	6	32	16	1	24	–	6	7	8
AH	—	—	—	16	19	59	—	—	6
AH3F4	—	—	—	13	19	61	—	—	7
BS	8	22	16	—	25	—	10	12	7
BH	—	—	—	8	25	58	—	—	9
BH3	—	—	—	14	26	54	—	—	6
BH4	—	—	—	10	19	63	—	—	8
BH6	—	—	—	12	22	59	—	—	7
BH3F4	—	—	—	12	24	59	—	—	5
CS	26	5	16	1	23	—	4	18	7
CS3	25	4	22	1	29	—	4	10	5
CS4	26	3	22	1	21	—	13	9	5
CS6	25	2	21	—	27	—	14	2	9
CS34	23	2	24	—	24	—	11	11	5
CS3F4	31	3	16	—	21	—	19	6	4
CSS19	14	1	17	—	13	—	22	27	6
DS	29	1	17	1	22	—	5	19	6
DS3	31	1	10	—	20	—	19	13	6
DS4	32	2	19	1	23	—	7	12	4
DS6	33	1	16	1	21	—	14	7	7
DS34	26	—	21	1	20	—	17	10	5
DS3F4	32	1	15	—	20	—	18	9	5
DSS19	12	—	15	4	11	—	14	38	6

TABLE 5 : Metallographic estimate of the percentage of different microstructural

SAMPLE	GROUP A	GROUP B	GROUP C	GROUP D
S	58.1	58.1	62.6	57.9
H	35.1	38.8	X	X
3	37.8	43.1	56.3	57.5
4	35.1	42.0	66.6	71.5
6	29.6	38.8	52.4	63.5
3-3	38.9	46.6	58.8	59.2
3-4	38.2	39.8	69.4	73.6
3-6	31.7	35.1	59.7	61.2
4-3	40.5	40.3	65.6	66.6
4-4	38.2	38.4	60.0	68.0
4-6	34.3	34.7	55.6	59.4
3F3	32.2	37.3	50.2	48.0
3F4	32.0	34.8	58.5	60.7
3F6	30.5	30.7	53.2	45.6
4F3	36.3	39.7	52.6	63.8
4F4	33.2	36.7	50.9	65.3
4F6	30.7	30.9	43.5	58.3

Sintering Furnace Belt Speed = 2 minutes / foot

TABLE 3 : Room temperature unnotched Charpy impact values (Joules) - specification = 27.2 J minimum .

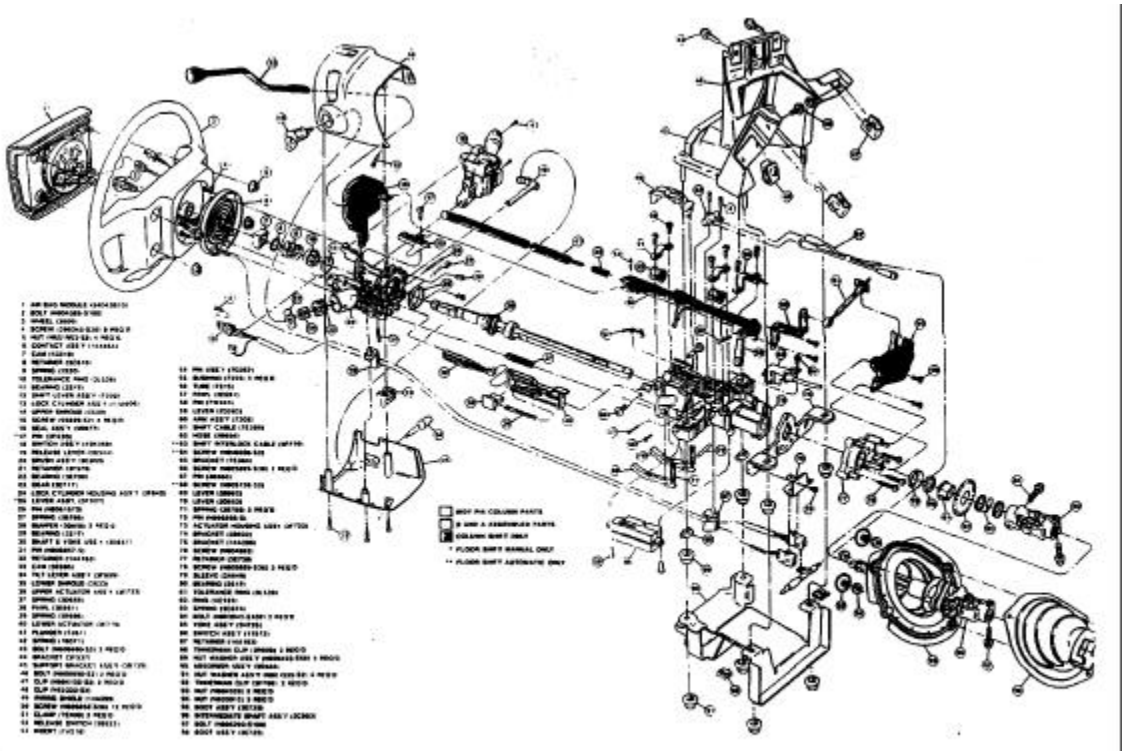

FIGURE 1 : Exploded view (schematic) of the steering column in which the tilt levers (part numbers 69 and 70) are used .

FIGURE 2 : Photograph of the tilt levers used in the steering column .

MICROHARDNESS (HV_{20})					
P	F	Fnr	NR	DM	LM
207	72	170	208	318	339

FIGURE 3 : Photomicrograph of sample BS (as-sintered , 0.3% graphite addition) . Etched with a combination of 2% nital/4% picral . Magnification 750X .
(P = pearlite , F = ferrite , Fnr = nickel rich ferrite , NR = nickel rich non-etching , DM = dark etching martensite , LM = light etching martensite)

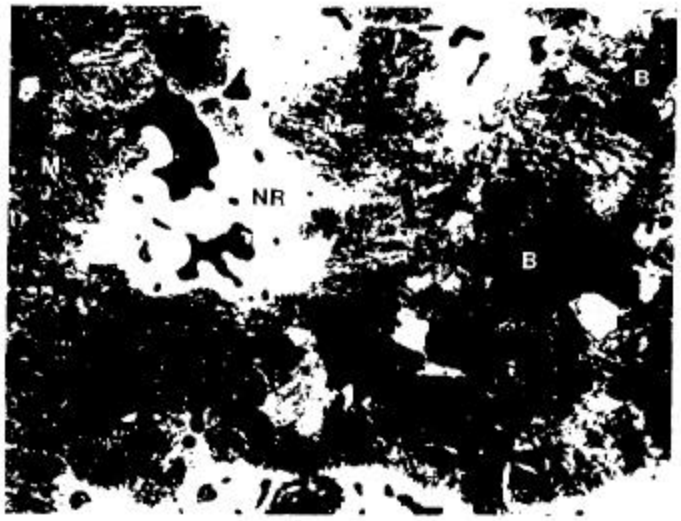

MICROHARDNESS (HV_{20})		
B	NR	M
197	149	401

FIGURE 4 : Photomicrograph of sample BH4 (quench-hardened , 0.3% graphite addition) . Etched with a combination of 2% nital/4% picral . Magnification 750X .
(B = bainite , NR = nickel rich non-etching , M = martensite)

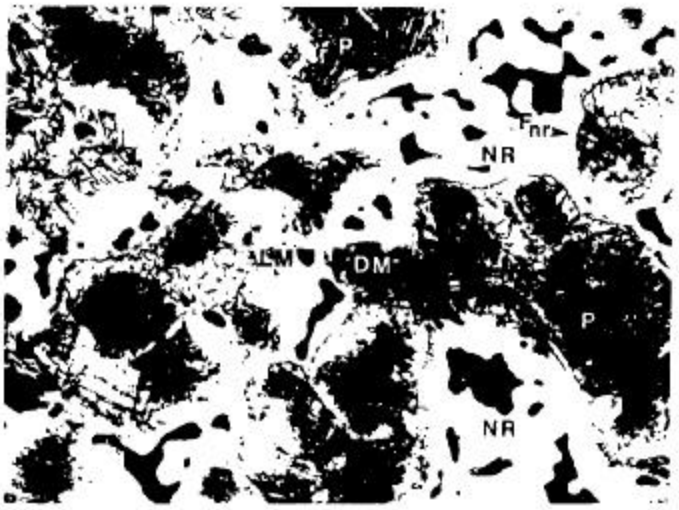

MICROHARDNESS (HV_{20})				
P	F_{nr}	NR	DM	LM
238	242	141	492	385

FIGURE 5 : Photomicrograph of sample DS4 (sinter-hardened , 0.8% graphite addition) . Etched with a combination of 2% nital/4% picral . Magnification 750X .
(P = pearlite , F_{nr} = nickel rich ferrite , NR = nickel rich non-etching , DM = dark etching martensite , LM = light etching martensite)

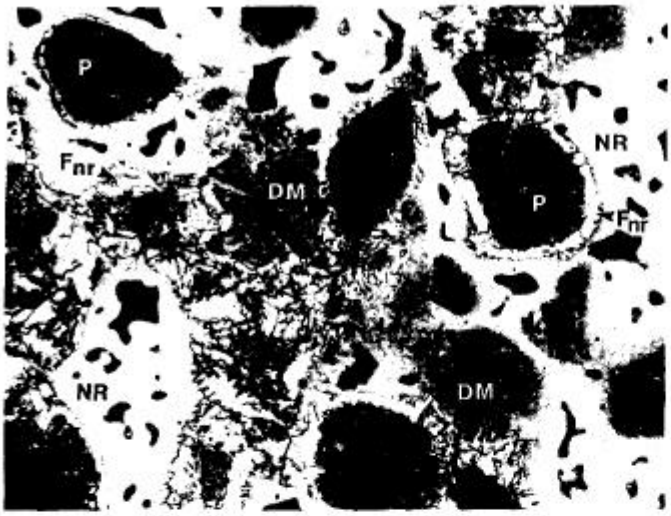

MICROHARDNESS (HV_{20})				
P	F_{nr}	NR	DM	LM
258	237	144	484	419

FIGURE 6 : **Photomicrograph of sample DS3-F-4 (sinter-hardened , 0.8% graphite addition) . Etched with a combination of 2% nital/4% picral. Magnification 750X .**
(P = pearlite , F_{nr} = nickel rich ferrite , NR = nickel rich non-etching , DM = dark etching martensite , LM = light etching martensite)

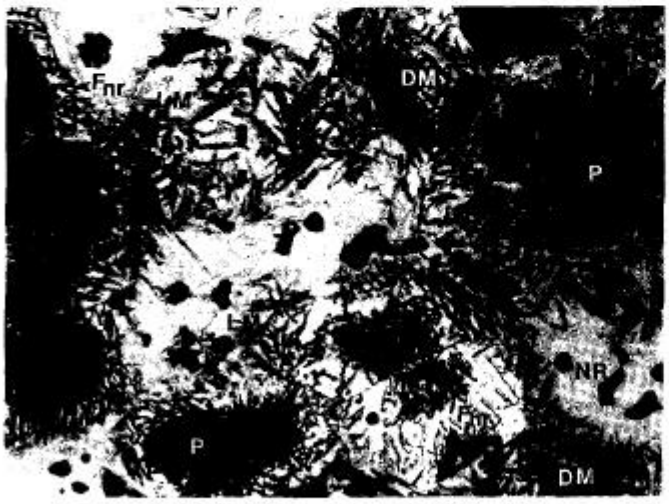

MICROHARDNESS (HV_{20})				
P	F_{nr}	NR	DM	LM
262	287	139	635	442

FIGURE 7 : **Photomicrograph of sample DSS19 (sinter-hardened , 0.8% graphite addition , extended sintering time) . Etched with a combination of 2% nital/4% picral . Magnification 750X .**
(P = pearlite , F_{nr} = nickel rich ferrite , NR = nickel rich non-etching , DM = dark etching martensite , LM = light etching martensite .

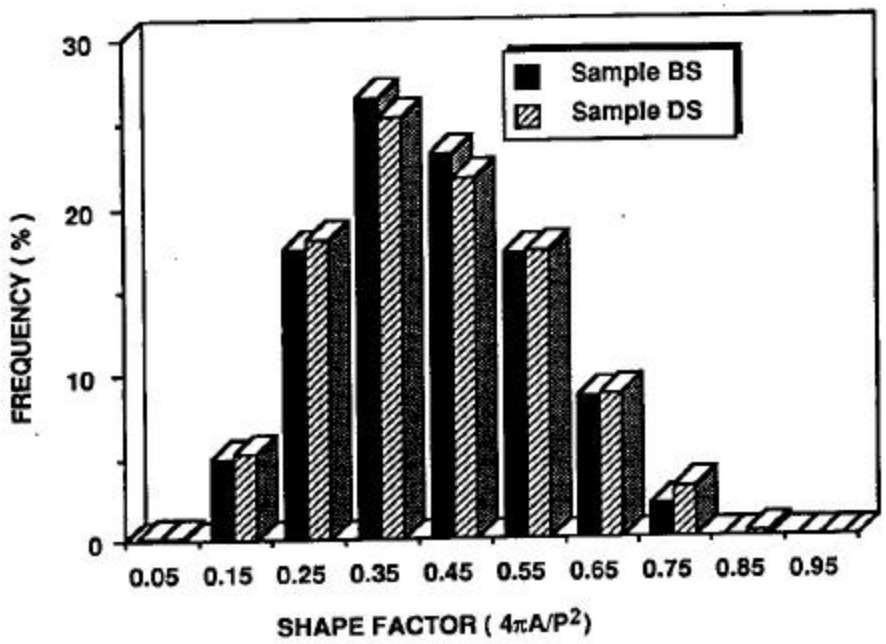

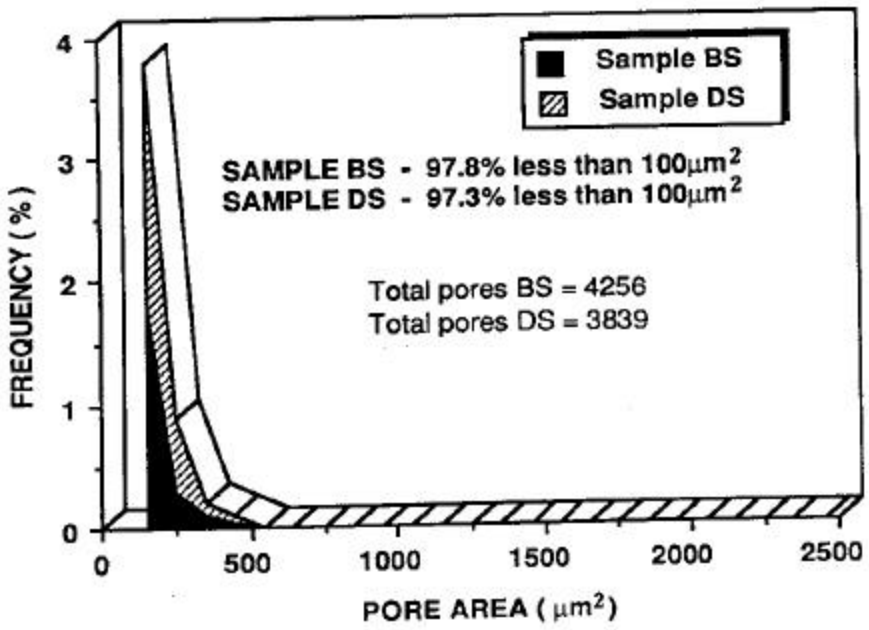

FIGURE 8 : Pore shape and pore size for samples BS and DS .

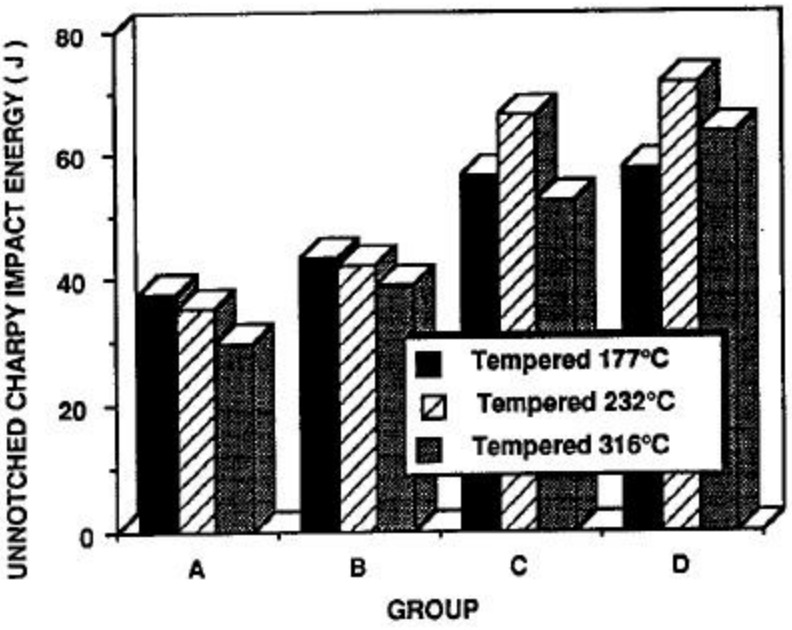

FIGURE 9 : Unnotched Charpy impact performance of single tempered samples from groups A , B , C , and D .

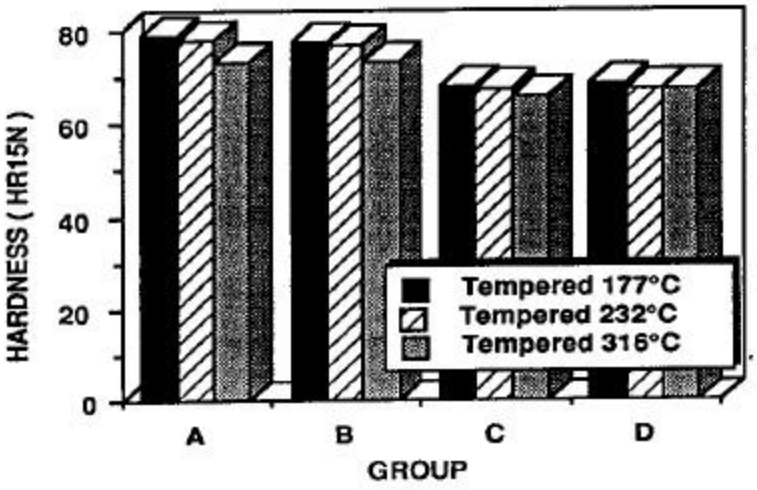

FIGURE 10 : Hardness (HR15N) of single tempered samples from groups A , B , C , and D .

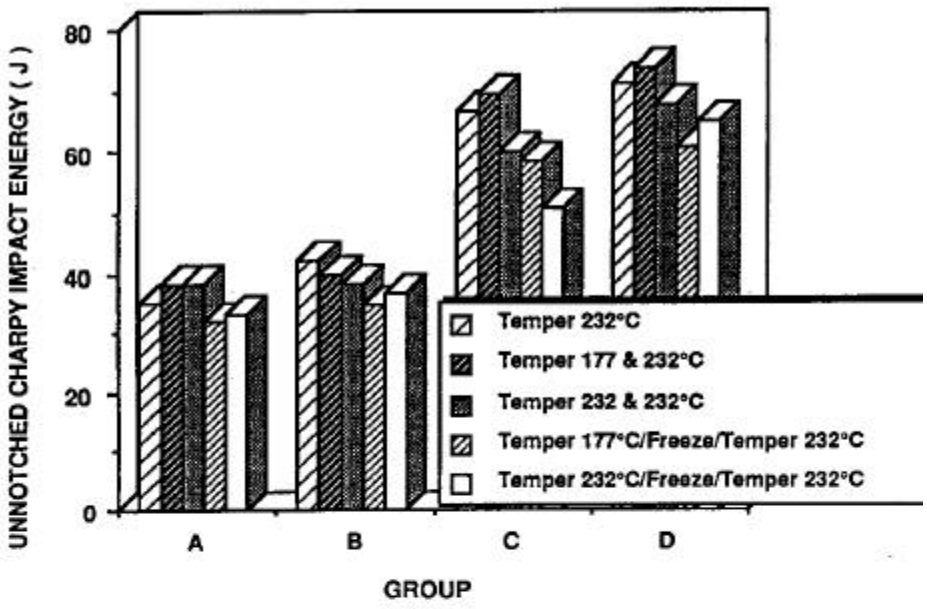

FIGURE 11 : The effect of different tempering and cryogenic treatments on the unnotched Charpy impact performance of samples from groups A , B , C , and D .

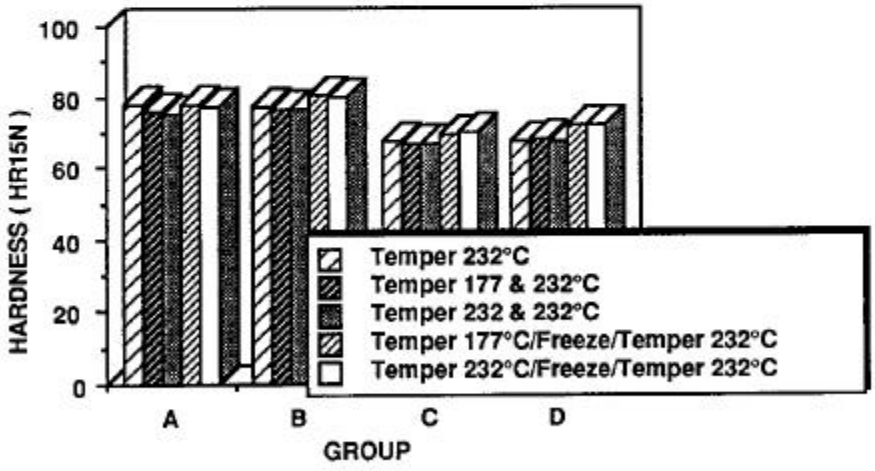

FIGURE 12 : The effect of different tempering and cryogenic treatments on the hardness (HR15 N) of samples from groups A , B , C , and D .

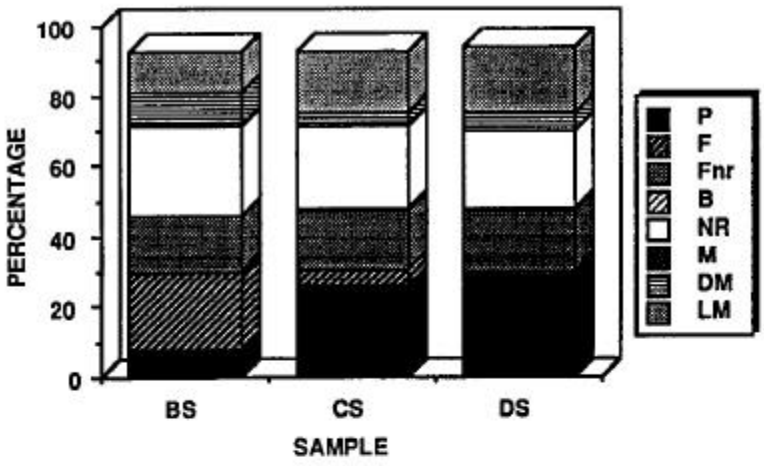

FIGURE 13 : The percentage of different microstructural constituents in as-sintered samples BS , CS ,and DS . (P = pearlite , F = ferrite , Fnr = nickel rich ferrite , B = bainite , NR = nickel rich non-etching , M = martensite , DM = dark etching martensite , LM = light etching martensite) .

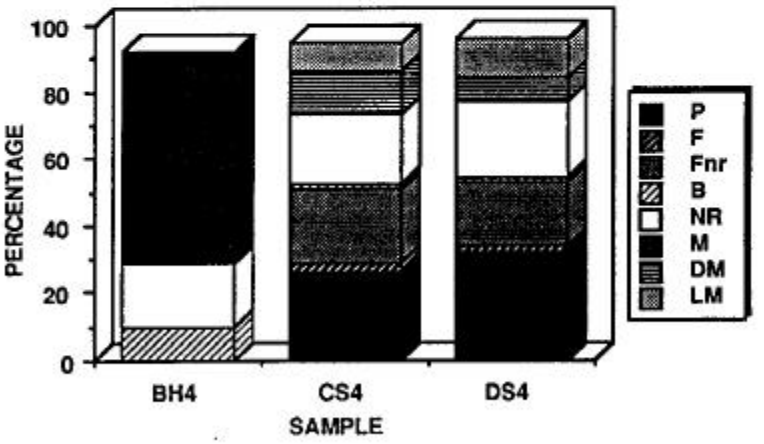

FIGURE 14 : The percentage of different microstructural constituents in single tempered samples BH4 , CS4 , and DS4 . (P = pearlite , F = ferrite , Fnr = nickel rich ferrite , B = bainite , NR = nickel rich non-etching , M = martensite , DM = dark etching martensite , LM = light etching martensite) .

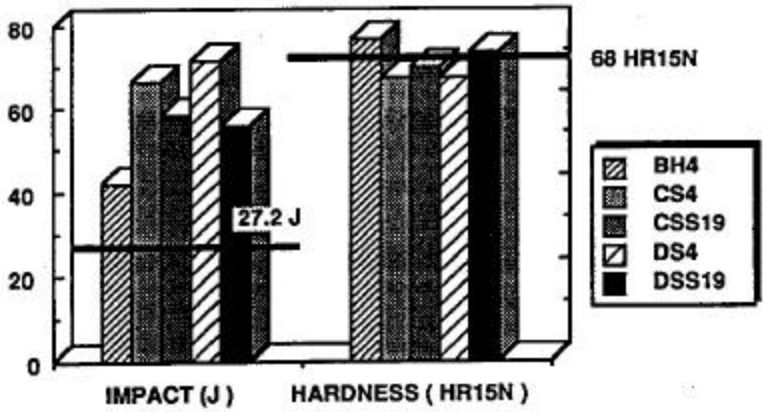

FIGURE 15 : The impact performance and hardness of single tempered samples BH4 , CS4 , CSS19 , DS4 , and DSS19 . Samples CSS19 and DSS19 were given an extended sinter compared with samples BH4 , CS4 , and DS4 .

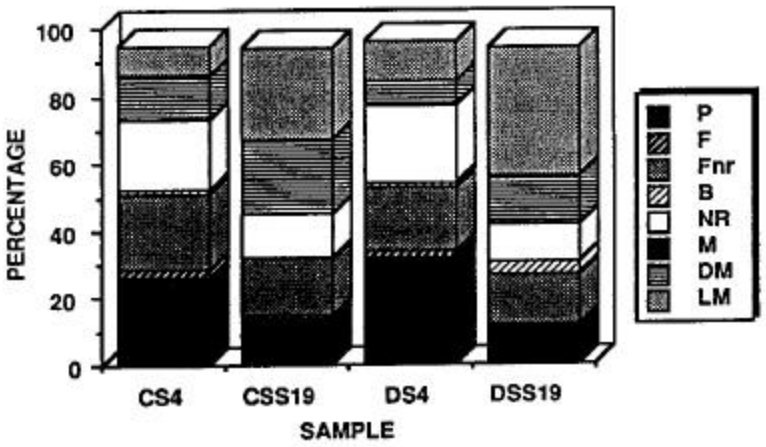

FIGURE 16 : The percentage of different microstructural constituents in sinter-hardened samples CS4 , DS4 , CSS19 , and DSS19 . Samples CSS19 and DSS19 were given an extended sinter compared with samples CS4 and DS4 . (P = pearlite , F = ferrite , Fnr = nickel rich ferrite , B = bainite , NR = nickel rich non-etching , M = martensite , DM = dark etching martensite , LM = light etching martensite) .

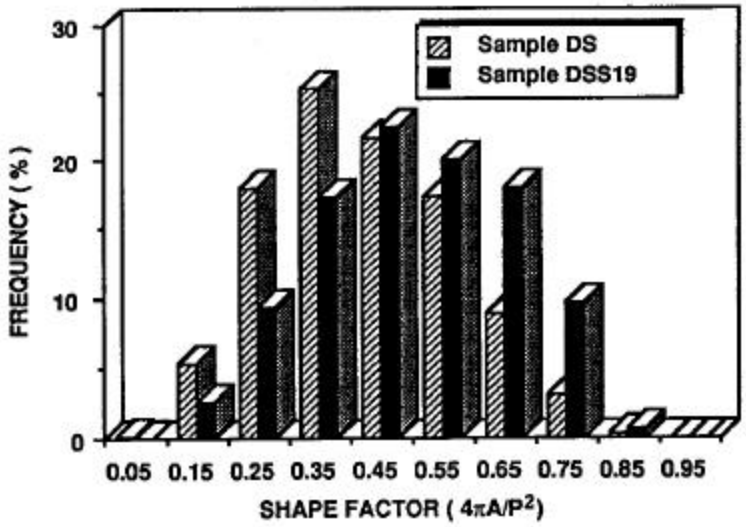

FIGURE 17 : Pore shape for samples DS and DSS19 .

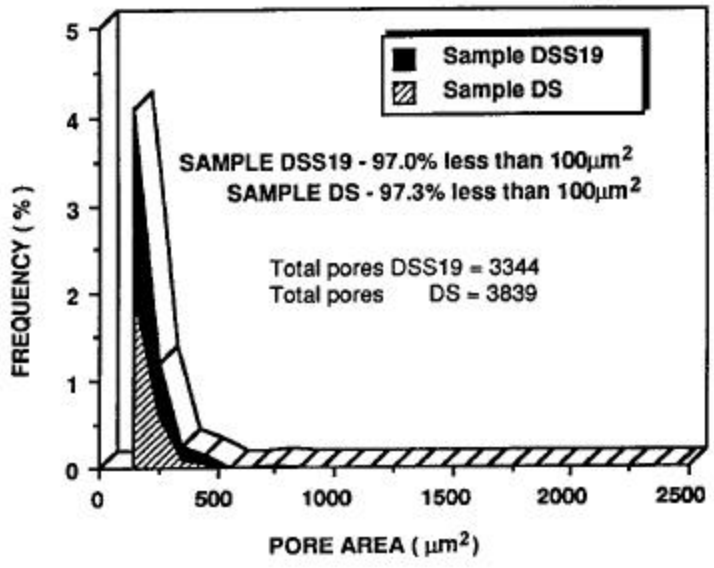

FIGURE 18 : Pore size for samples DS and DSS19 .